Available online at www.sciencedirect.com
ScienceDirect
European Polymer Journal 44 (2008) 189–199
EUROPEAN POLYMER JOURNAL
www.elsevier.com/locate/europolj

Morphology of polystyrene-*block*-poly(styrene-*co*-acrylonitrile) and polystyrene-*block*-poly(styrene-*co*-acrylonitrile-*co*-5-vinyltetrazole) diblock copolymers prepared by nitroxide-mediated radical polymerization and "click" chemistry

Daniel Gromadzki [a], Jan Lokaj [a], Peter Černoch [a,*], Olivier Diat [b], Frédéric Nallet [c], Petr Štěpánek [a]

[a] *Institute of Macromolecular Chemistry, Academy of Sciences of the Czech Republic, Heyrovsky Sq. 2, 162 06 Prague 6, Czech Republic*
[b] *Structure et Propriétés d'Architectures Moléculaires, UMR 5819 (CEA-CNRS-UJF), DRFMC/SPrAM, CEA-Grenoble, 38054 Grenoble cedex 9, France*
[c] *Centre de Recherches Paul-Pascal, CNRS, avenue du Docteur-Schweitzer, F-33600 Pessac, France*

Received 29 May 2007; received in revised form 17 October 2007; accepted 30 October 2007
Available online 13 November 2007

Abstract

Well-defined polystyrene-*block*-poly(styrene-*co*-acrylonitrile) PS-*block*-P(S-*co*-AN) and poly(styrene-*co*-acrylonitrile-*co*-5-vinyltetrazole) PS-*block*-P(S-*co*-AN-*co*-5VT) block copolymers with various content of acrylonitrile units in the statistical block were synthesized by nitroxide mediated radical polymerization (NMRP) and post-functionalized using efficient "click" chemistry process. In the second step, acrylonitrile units were successfully modified using 1,3-dipolar cycloaddition ("click" chemistry) type polymer analogue reaction. The original pristine diblock copolymers can be molecularly dissolved in THF and dioxane while the "tetrazolated" versions aggregate to clusters as determined by dynamic light scattering (DLS). Small-angle X-ray scattering (SAXS) and Transmission Electron Microscopy (TEM) revealed ordered lamellar morphology with interlamellar spacing $d = 60$ nm increasing to $d = 80$ nm for "tetrazolated" diblock copolymers. The morphological features of diblock copolymer thin layers observed by Atomic Force Microscopy (AFM) depend on the tunable content of both acrylonitrile and 5-vinyltetrazole units and on the quality (polarity) of the solvents used.

Keywords: Polystyrene-*block*-poly(styrene-*co*-acrylonitrile-*co*-5-vinyltetrazole); TEMPO; "Click" chemistry; Morphology; Membrane

1. Introduction

Excellent properties of poly(styrene-*co*-acrylonitrile) copolymers (P(S-*co*-AN)) such as chemical resistance, thermal stability and processability make them attractive for a wide range of applications. Conventional radical polymerization of styrene and acrylonitrile yields copolymers with broad molecular weight distributions and ill-defined structure. On the other hand controlled radical polymerization techniques such as nitroxide mediated radical polymerization (NMRP) [1], atom transfer

* Corresponding author. Tel.: +420 296 809 296; fax: +420 296 809 410.
E-mail address: pcernoch@imc.cas.cz (P. Černoch).

0014-3057/$ - see front matter © 2007 Elsevier Ltd. All rights reserved.
doi:10.1016/j.eurpolymj.2007.10.029

radical polymerization (ATRP) [2] and reversible addition fragmentation chain transfer (RAFT) [3] provide a synthetic tool for making polymers with required molecular weight, well-defined compositions and complex architectures. Living radical polymerization producing PS-*b*-P(S-*co*-AN) block copolymers by NMRP [4–6], ATRP [7–9] and RAFT [10,11] methods have been reported. Fukuda first synthesized PS-*b*-PSAN block copolymers by copolymerization of S–AN mixture initiated with nitroxide-terminated polystyrene [4]. As the nitroxide, a commercially available stable radical TEMPO was applied. Baumert and Mülhaupt prepared PS-*b*-P(S-*co*-AN) block copolymers with carboxylic end-functionality; its fraction in the P(S-*co*-AN) block corresponded to 0.19, 0.37 and 0.42 [12]. Bauman et al. extended the studies on PS-*b*-P(S-*co*-AN) block copolymers by varying the monomer ratio in the feed in the presence of TEMPO radical as a controller [13]. Recently, a series of PS-*b*-PSAN copolymers with an azeotropic composition of PSAN blocks were synthesized by TEMPO-mediated radical polymerization and the permeabilities of the film-forming products were measured [14]. PS-*block*-PAN copolymers were also synthesized by combination of living anionic and controlled radical ATRP methods [15]. It was achieved by preparing first the polystyrene block, converting the end group to bromine initiating site for ATRP process and chain extension with acrylonitrile block.

There is currently significant interest not only in the synthesis of new polymeric materials but also in the modification of existing polymers in order to impart new properties and meet requirements for new applications. Chemical modification of styrene–acrylonitrile copolymers is a rather new topic in the field of polymer chemistry. Acrylonitrile units incorporated in polymer chains offer possibilities of introducing desirable physical and chemical properties to the polymer material. Polymers containing ionic functions are particularly interesting as ion-exchange and chelating materials.

Detailed studies have been devoted to alkaline hydrolysis of polyacrylonitrile [16–18] as well as P(S-*co*-AN) copolymers [19]. High conversion of acrylonitrile units to acrylamide and carboxylic groups in polyacrylonitrile was achieved, however, the PSAN copolymers showed considerable resistance toward the alkaline hydrolysis. Hseish et al. developed a procedure for transformation of acrylonitrile to oxazoline functionality in P(S-*co*-AN) copolymers [20,21]. Due to high reactivity of the oxazoline functionality, the modified P(S-*co*-AN) copolymers can be used as compatibilizers in reactive blending with polymers bearing complementary functional groups such as polyamides and polyterephthalates. Similar investigations concerning transformation of acrylonitrile units to reactive oxazoline functionality and further to oxazolium salts by ring opening reaction were described [22,23].

Some efforts have been paid to chemical modification of polyacrylonitrile with different amines [24] and hydroxylamines with the aim to develop chelating materials (resins, fibres) capable to form complexes with metals via hydrogen bonding [25]. The modification of styrene–acrylonitrile networks with hydroxylamine yielded chelating ion-exchanging resins [26].

Gaponik et al. carried out extensive studies on transformation of polyacrylonitrile into poly(5-vinyltetrazole) [27]. High conversions up to about 95% were achieved and further modifications, i.e., alkylation of the obtained products, were demonstrated [28]. More recently, chemical modification of polyacrylonitrile with sodium azide was undertaken by Huang [29]; also in this case conversions to 5-vinyltetrazoles as high as 98% were reported. Ulbricht et al. used azides substituted with hydrophobic and hydrophilic groups for photochemical modification of polyacrylonitrile ultrafiltration membranes [30]. The 1,3-dipolar cycloaddition reaction on P(S-*co*-AN) copolymers leading to 1,2,4-oxadiazoles were reported by Paton et al. [31].

The Huisgen 1,3-dipolar cycloaddition [32], which is ranked among "click" chemistry reactions due to its high efficiency and tolerance to various functional groups, proved to be very practical and efficient in organic synthesis [33,34]. The "click" reactions are extensively explored for the synthesis of polymers of various type and architecture [35–47], chemical modification of preformed (co)polymers [48–53] or as a convenient method for preparation of end-functional polymers [54,55].

Polymers containing weak acidic 5-vinyltetrazole function may find numerous applications ranging from biomedicine (construction of drugs), absorbents, hydrogels or coordinating agents. The 5-vinyltetrazole functionality can be made both anion conductive by quaternization reactions or proton conductive by acid doping offering a way to prepare polymer electrolyte membranes (PEMs) for fuel cell devices [56]. Many other chemical transformations involving 5-vinyltetrazole functionality leading to

new functional materials has been recently reported or reviewed [57,58].

The present study is aimed at describing the solution and bulk behavior of well-defined amphiphilic diblock copolymers polystyrene-*block*-poly(styrene-*co*-acrylonitrile) and polystyrene-*block*-poly(styrene-*co*-acrylonitrile-*co*-5-vinyltetrazole).

2. Experimental part

2.1. Materials

Styrene (Kaučuk Group Co., Kralupy, Czech Republic) and acrylonitrile (Fluka) were distilled under reduced pressure prior to use. Sodium azide and zinc chloride were commercial products of Aldrich. TEMPO (2,2,6,6-tetramethylpiperidin-1-yloxyl radical) and dibenzoyl peroxide were of Fluka. The solvents used were of analytical grade.

2.2. Synthesis and chain extension of TEMPO-terminated polymer macroinitiators

The procedure for the synthesis of both a poly(S-*co*-AN) macroinitiator or TEMPO-terminated polystyrene and related diblock copolymers comprising polystyrene and S–AN copolymer blocks was described earlier [4,13]. Chain extension of the P(S-*co*-AN) copolymer macroinitiator D1 with styrene produced a diblock copolymer DB1, the S–AN copolymerization, initiated with the TEMPO-terminated polystyrene (PS), yielded diblock copolymers DB2 and DB3. In the preparation of DB2, an azeotropic mixture of styrene (63 mole%) and acrylonitrile (37 mole%) was used; in the case of DB3, the feed contained 20 and 80 mole%, respectively, of styrene and acrylonitrile.

The contents of styrene and acrylonitrile units in the synthesized copolymers were determined by elemental analysis. Using a PS as a macroinitiator in the S–AN copolymerization, the dependence of the copolymer composition on the feed composition derived from the published monomer reactivity ratios r ($r_S = 0.49$ and $r_{AN} = 0.04$) was employed for the determination of the mole ratio of S and AN in the formed P(S-*co*-AN) blocks.

Molecular weights were measured by SEC. The M_n values of diblock copolymers, containing the generated P(S-*co*-AN) blocks, attached to the completely consumed PS macroinitiator, were also calculated according to

$$M_n = 3.86 \times 10^4\{1 + [(f_S)_2 \times M_S]/[(f_S)_1 \times M_S] + [f_{AN} \times M_{AN}]/[(f_S)_1 \times M_S]\}, \quad (1)$$

where 3.86×10^4 is the number-average molecular weight of the macroinitiator PS, $(f_S)_1$ and $(f_S)_2$ are the mole fractions of styrene units from both the macroinitiator and the formed poly(S-*co*-AN) block, f_{AN} corresponds to the mole fraction of AN units in the diblock copolymer, M_S and M_{AN} are molecular weights of S and AN, respectively. Table 1 presents some characteristics of the prepared macroinitiators and block copolymers.

2.3. Modification of polystyrene-block-poly(styrene-co-acrylonitrile) diblock copolymers to polymers containing 5-vinyltetrazole units

The modification of acrylonitrile (Fig. 1) in the block copolymers were performed according to

Table 1
Characteristics of the synthesized TEMPO-terminated polymer macroinitiators (PS, D1) and related diblock copolymers (DB1, DB2, DB3)

Polymer	$M_n \times 10^{-4}$ [a]			M_w/M_n	$(f_S)_1$	f_{AN}	(f_{AN})
	_[b]	_[c]	_[d]				
PS	–	3.86	–	1.08	–	–	–
D1	–	–	0.95	1.34	–	–	0.19
DB1	2.74	1.79	0.95	1.56	0.65	0.08	0.19
DB2	7.07; 10.06[e]	3.86	3.21; 6.20[e]	1.45	0.34	0.25	0.37
DB3	8.7; 10.40[e]	3.86	4.84; 6.54[e]	1.17	0.30	0.35	0.51

$(f_S)_1$ is the mole fraction of styrene units from the PS macroinitiator, incorporated in the diblock copolymer, f_{AN} and (f_{AN}) are the mole fractions of acrylonitrile units in the diblock copolymer and in the corresponding poly(styrene-*co*-acrylonitrile) block, respectively.

[a] Polystyrene-equivalent molecular weight; SEC.

[b] The value relates to the diblock copolymer.

[c] The value relates to the polystyrene block.

[d] The value relates to the poly(styrene-*co*-acrylonitrile) block.

[e] The value was calculated from both the M_n of PS (3.86×10^4) and the copolymer composition.

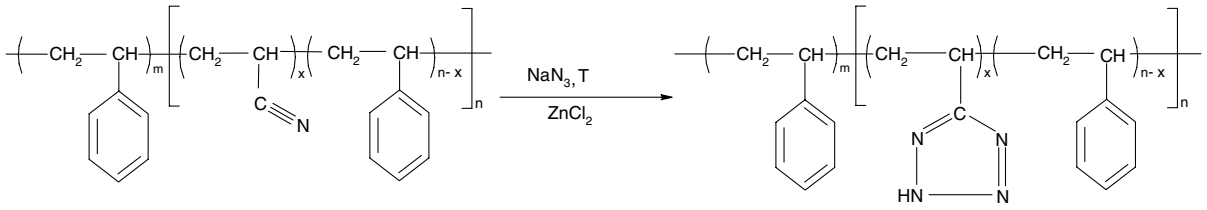

Fig. 1. Transformation of polystyrene-*block*-poly(styrene-*co*-acrylonitrile) copolymers into polystyrene-*block*-poly(styrene-*co*-acrylonitrile-*co*-5-vinyltetrazole) using 1,3-dipolar cycloaddition (“click” chemistry) type polymer analogue reaction.

previously reported procedures [26,28,43]. The reaction of PS-*b*-P(S-*co*-AN) with sodium azide and zinc chloride was carried out in a round-bottomed flask equipped with a stirrer, thermometer and a reflux condenser. To a 5–10 wt.% solution of PS-*b*-P(S-*co*-AN) in dimethylformamide (DMF) was added a fourfold excess of NaN_3, and the catalyst $ZnCl_2$ was added (in the DB3 modification, NH_4Cl was used as a catalyst); the reaction mixture was stirred at 120 °C for 48 h. An increased temperature and a long reaction time favored the modification efficiency. The obtained products were purified by pouring the reaction mixture into a diluted HCl solution. The final product was recovered by filtration and dried under vacuum at 50 °C for two days.

Using FT-IR spectroscopy, the process of “tetrazolation” was followed by the disappearance of nitrile signal at 2237 cm^{-1} (C≡N stretching vibrations). The presence of the resulting 5-vinyltetrazole groups was evidenced by the characteristic tetrazole bands at 3000–3400 cm^{-1} (associated N—H), 2300–2800 cm^{-1} (N^+—H) and 1555 cm^{-1} (C=N).

The degree of modification (D_M), i.e., the conversion of AN units into 5-vinyltetrazole units, was expressed by the ratio of weight fractions of incorporated N_3H (w_T) in the partly and completely modified block copolymer, namely, by $w_T/(w_T)_C$. The values w_T, $(w_T)_C$ and the weight fraction of total acrylonitrile units (both unreacted and transformed with N_3H) in the modified block copolymer (w_{AN}) were available from data comprising the molecular weights of acrylonitrile (M_{AN}), N_3H (M_T) and nitrogen contents in N_3H (N_T), AN (N_{AN}), in the original (N_O) and modified (N_M) block copolymer:

$$w_T = (N_M - N_O)/(N_T - N_O), \quad (2)$$

$$(w_T)_C = w_{AN} \times (M_T/M_{AN}), \quad (3)$$

$$w_{AN} = (1 - w_T) \times (N_O/N_{AN}) = [(N_T - N_M)/(N_T - N_O)] \times (N_O/N_{AN}). \quad (4)$$

For the calculation of the D_M values, Eq. (5) was employed:

$$D_M = [(N_M - N_O)/(N_T - N_M)] \times (N_{AN}/N_O) \times (M_{AN}/M_T). \quad (5)$$

The results of the modification of the synthesized block copolymers are given in Table 2.

2.4. Characterization methods

Polymer molecular weights were estimated using SEC instrument: Deltachrom pump (Watrex Comp.), autosampler Midas (Spark Instruments, The Netherlands), two columns with PL gel MIXED-B LS (10 μm), separating in the M_n range 4×10^2–10×10^6. Dawn-DSP-F laser light scattering (MALLS) photometer (Wyatt Technology Corp., USA) and Shodex RI-71 refractive index detector (Japan) were used as detectors. The instrument was calibrated with linear monodisperse polystyrene (PS) standards (Polymer Standard Service, Mainz, Germany), the eluent being THF. The injection-loop volume was 0.1 mL. The data were accumulated and processed using Astra Software 4.70.07.

The copolymer compositions were found from nitrogen analysis with available elemental analysis instrumentation.

Table 2
Results of the modification of polystyrene-*block*-poly(styrene-*co*-acrylonitrile) diblock copolymers (DB1, DB2, DB3) with N_3H

Sample designation	Copolymer	Nitrogen content (%)	Degree of modification (D_M) (%)
DB1	DB1	1.18	–
DB1T	P(S-*co*-AN-*co*-5VT)	1.41	20
DB2	DB2	3.80	–
DB2T1	PS-*b*-P(S-*co*-AN-*co*-5VT)	7.54	36
DB2T2	PS-*b*-P(S-*co*-AN-*co*-5VT)	10.50	66
DB2T3	PS-*b*-P(S-*co*-AN-*co*-5VT)	12.76	82
DB3	DB3	5.75	–
DB3T	PS-*b*-P(S-*co*-AN-*co*-5VT)	16.04	71

IR spectra of the polymers in the form of KBr pellets were taken on Perkin–Elmer Paragon 1000PC infrared spectrometer. Carbon, hydrogen, nitrogen and iodide content were determined with available elemental analysis instrumentation.

2.5. Dynamic light scattering (DLS)

Solutions in THF of the polymers have been investigated by dynamic light scattering (DLS) using an ALV CGE photogoniometer equipped with a Uniphase 22 mW HeNe laser and an ALV6010 correlator. The measured intensity correlation curves $g^2(t)$ were converted into distributions $A(\tau)$ of relaxation times τ using the inverse Laplace transformation

$$g^2(t) = 1 + \beta\left[\int A(\tau)\exp(-t/\tau)\,\mathrm{d}\tau\right]^2, \quad (6)$$

where t is the delay time of the correlation function and β an instrumental parameter. The programme REPES [59] was used to perform the inverse Laplace transformation in Eq. (6). The relaxation time τ is related to the diffusion coefficient D by the relation $D = (\tau q^2)^{-1}$ where q is the scattering vector. The hydrodynamic radius R_H of the particles is calculated from the diffusion coefficient using the Stokes–Einstein equation:

$$D = k_B T/6\pi\eta R_H, \quad (7)$$

where T is absolute temperature, η the viscosity of the solvent and k_B the Boltzmann constant. By a similar procedure, the distribution of relaxation times $A(\tau)$ can be transformed into a distribution of hydrodynamic radii $A(R_H)$, to be used below.

2.6. Small angle X-ray scattering (SAXS)

SAXS measurements have been performed on two different instruments to cover a wide range of scattering vectors. For a part of the samples a Nanostar-U instrument was used (Bruker AXS) with Goebel mirrors and a HiSTAR 2D detector positioned 1070 mm from the sample. For other samples a Nonius FR591RAG rotating anode was used coupled with a home-made optical set-up with a long collimation and a 2D gas-filled detector located at 3600 mm from the sample to reach values of scattering vector q as small as $q = 2 \times 10^{-3}$ Å^{-1} ($q = (4\pi/\lambda)\sin(\theta/2)$ and θ is the scattering angle). Both X-ray sources were a Cu-anode source yielding a beam with wavelength $\lambda = 1.54$ Å. The resulting 2D images were found in all cases to be isotropic; the data were azimuthally averaged to yield intensity vs. q scattering curves. The scattering experiments were performed at room temperature. The polymer samples were either sealed in 2-mm capillaries, which were placed in the evacuated chamber of the instrument or inserted in a cell with thin Kapton windows. Usual corrections for background subtraction and detector response were applied.

2.7. Transmission electron microscopy (TEM)

TEM measurements were performed on a microscope JEM 200CX (Jeol, Japan). All microphotographs were taken at acceleration voltage 100 kV and recorded with a digital camera. Brightness, contrast and gamma corrections were performed with standard software. Ultrathin sections of ca. 50 nm were cut from the thermo-annealed bulk sample with the ultramicrotome Leica Ultracut UCT, equipped with cryo attachment. Temperatures during cutting were −110 °C and −50 °C for the sample and the knife, respectively. The samples were stained with RuO_4 to obtain contrast images.

2.8. Atomic force microscopy (AFM)

AFM imaging has been performed with a multimode AFM Nanoscope IIIa (Digital Instruments) in tapping mode. This method allows to obtain both topography and phase scans of explored surfaces, so after measurement we have information about the surface topography profile (given by profile image) and surface domains arrangement (visible in phase image). For scanning we use BS-Tap300-50 tips (Nanoscience Instruments) with resonant frequency about 300 kHz and tip radius <10 nm. The measured data were processed with software WSxM® (Nanotec Electronica; http://www.nanotec.es).

3. Results and discussion

3.1. Dynamic light scattering

Dilute solutions of all three copolymers DB1, DB2, DB3 have been examined by dynamic light scattering. The solvent used was THF as a good solvent for both blocks. Fig. 2a shows the distribution of sizes obtained from the measured correlation functions using Eqs. (6) and (7). In all cases the distributions are unimodal showing that the polymer is fully dissolved. From the position of the peak in

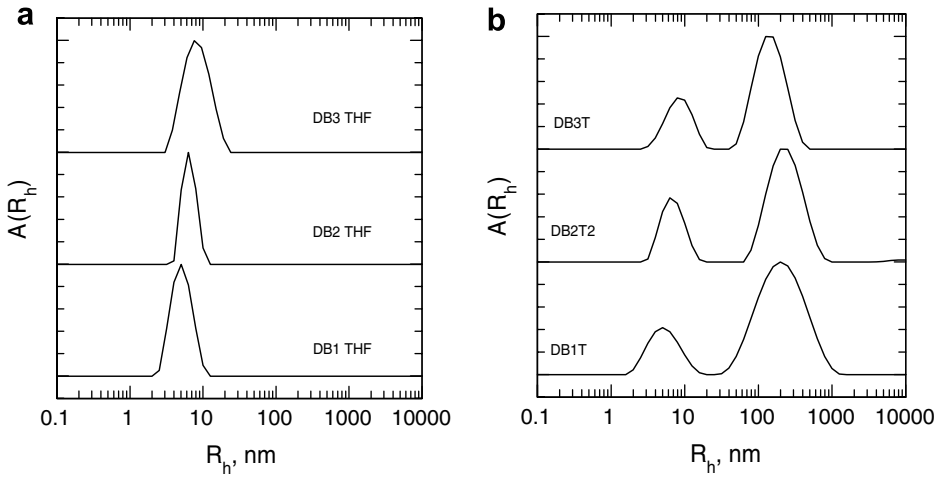

Fig. 2. Distributions $A(R_H)$ of hydrodynamic radii of (a) the diblock copolymers and (b) their tetrazolated versions, dissolved in THF.

Fig. 2a we can calculate the hydrodynamic radius of the polymer, R_H. The results are compiled in Table 3. The size of the polymer increases with increasing molecular weight. Fig. 2b shows results for the same polymers after tetrazolation. All distribution functions are now bimodal, indicating the presence of small and large particles. The hydrodynamic radii of these particles are listed in Table 3.

The small particles have sizes very similar to the polymers before tetrazolation and represent therefore the molecularly dissolved polymer. The larger particles have a size in the average range 100–300 nm. They represent multimolecular clusters associated by interaction of polar tetrazole groups. The fact that we observe simultaneously the molecularly dissolved polymer and the clusters indicates that a certain density of tetrazolated units is needed on the acrylonitrile–styrene block.

Creation of the tetrazolated monomers on the polymer chains involves two random processes which lead to a certain heterogeneity in the distribution of the modified monomers among the polymer chains. The first random process is the copolymerization of the second block of the diblock copolymer, styrene with acrylonitrile. The second random process is the partial tetrazolation of the acrylonitrile units. This altogether means that statistically some chains will have a smaller number of monomers tetrazolated while the tetrazolation level of others will be significantly larger. While it is not possible to quantitatively assess the exact extent of variability in the tetrazolation level between the individual polymer chains, it is clear that chains which have a lower level of tetrazolation can remain molecularly dissolved, while chains with higher level of tetrazolation will aggregate in clusters, because the tetrazole units are insoluble in THF. The effect of tetrazolation on the cluster component is shown in Fig. 3 for the copolymer DB2. With increasing degree of tetrazolation the amplitude of the cluster component substantially increases, while the size of the clusters remains approximately constant, of the order of 200 nm. The clusters have a rather polydisperse size, indeed, e.g., Fig. 2b shows that the width of the cluster component is substantially larger than that corresponding to the molecularly dissolved polymer. A standard analytical fit (Pearson function) [61] into these two components shows a distribution width for the clusters, $\sigma_c = 0.34$ (corresponding to a molar mass polydispersity index $M_w/M_n = 8.3$, see Ref. [61]) while the width of the molecularly dissolved polymer is much smaller, $\sigma_c = 0.11$ (corresponding to $M_w/M_n = 1.20$).

Similar results were obtained for solutions of these polymers in dioxane (figures not shown): The original polymers were fully dissolved while the cluster component in the distributions of hydro-

Table 3
Hydrodynamic radii of the particles corresponding to the peaks in Fig. 2a and b

	$R_{h,1}$ (nm)	$R_{h,2}$ (nm)
DB1	4.9	5.0
DB2	6.4	6.8
DB3	8.3	8.6
DB1T	–	185
DB2T2	–	217
DB3T	–	165

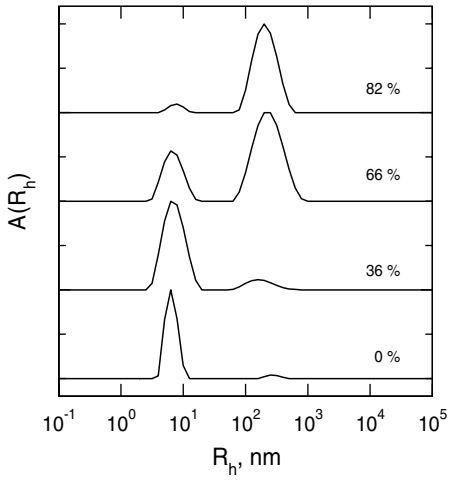

Fig. 3. Distributions of hydrodynamic radii for 1% THF solutions of the diblock copolymer DB2 with the indicated degree of tetrazolation.

dynamic radii for the tetrazolated polymers had substantially larger amplitude than in the case of THF solutions.

3.2. SAXS and TEM studies

The scattering profiles for all polymers exhibit the main structure peak positioned at q_0 and several side maxima located at multiples of q_0; an example is shown in Fig. 4. This indicates that the morphology of the polymers is lamellar, the characteristic lamellar distance d is approximately 60 nm as calculated from the relation $d = 2\pi/q_0$. Fig. 4 and Table 4 show that with increasing degree of tetrazolation d substantially increases, by about 25% for a 66% degree of tetrazolation. This is a consequence of replacement of the acrylonitrile unit by the bulkier vinyltetrazole unit and by the increased stiffness of the chain after tetrazolation. The fact that up to four diffraction orders can be observed on the X-ray scattering curves indicates that the lamellar morphology of the samples has a long-range regularity. The polymer sample however is not a "monocrystal", but has a grainy structure consisting of randomly oriented grains of material, each of them having the lamellar morphology. This is evidenced by the fact that the structural peaks corresponding to the lamellar structure are superimposed on a general decay $I(q) \sim q^{-4}$ as seen in Fig. 4. The slope -4 is given by the theoretical relations for scattering from grainy material [60]. The grainy nature of the material comes from the random spontaneous self-organization of the polymer during evaporation of the solvent in the membrane preparation process. The clusters of the more tetrazolated regions of the material that were observed in the solutions by DLS are not seen in these TEM figures because the solvent was removed by evaporation during the preparation of these bulk polymer samples.

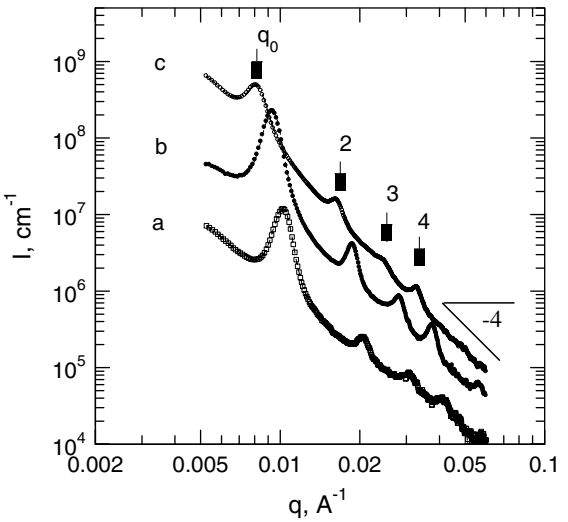

Fig. 4. X-ray scattering profiles $I(q)$ for the diblock copolymer DB2 (a) and its tetrazolated versions DB2T1 (b) and DB2T3 (c). The numbers show the expected peak positions at multiples of q_0. Curves (b) and (c) have been shifted vertically by 1 and 2 decades, respectively.

The X-ray scattering results are confirmed by the TEM images shown in Fig. 5. A good lamellar morphology is observed for all the samples and analysis of the images by the program ImageJ yields the lamellar distances shown in the last column of Table 4. They are in good agreement with the distances obtained by SAXS, the small differences between the two techniques are due to the fact that in TEM the lamellar structure can be slightly deformed by the preparation procedure and the cut of the sample may be not perpendicular to the lamellar planes.

Table 4
Lamellar period d derived from the position of q_0 for the samples shown in Fig. 4

Sample	Degree of tetrazolation (%)	d (nm)	
		SAXS	TEM
DB2	0	62.8	60
DB2T1	36	67.5	61
DB2T3	82	78.5	77

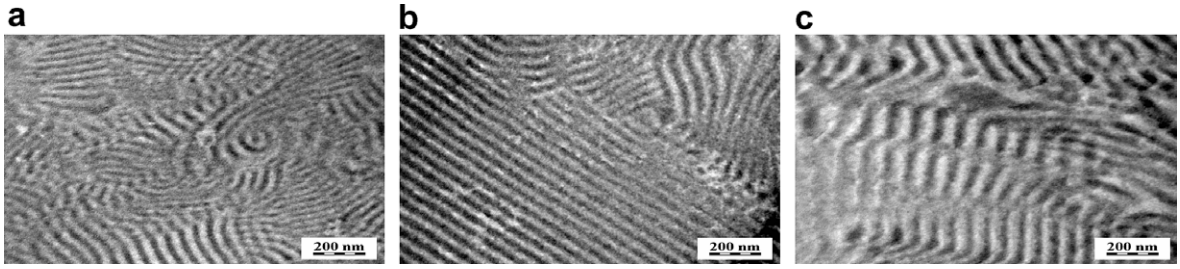

Fig. 5. TEM images of the polymers (a) DB2, (b) DB2T1, (c) DB2T3.

3.3. Atomic force microscopy experiments

Thin films for AFM measurements have been prepared by the spin-coating technique from stock solutions of the polymers at 1% concentration, on polished silica wafers. The solvents were THF (a good solvent for polystyrene and bad solvent for the tetrazolated units) and dioxane (a good solvent for polystyrene and moderately good for the tetrazolated units). We shall first examine thin layers of the original copolymers and then discuss the results of the tetrazolated samples.

Selected scans of the unmodified copolymers are shown in Fig. 6. In images (a)–(c) it is visible that the samples spun from THF demonstrate a marked tendency to form pore-like structured layers. Analysis of the sample DB1 (image a) yields an average diameter of holes ca. 1.1 μm, in the case of DB2 (image b) a diameter of ca. 200 nm. In a detailed study of the bottom part of these holes we did not find any other substructures (the tetrazolated polymers discussed below exhibit a different behavior), so the pores appear like regular cylindrical depressions in the layer topography. One can also conclude that with increasing molecular weight and content of acrylonitrile in the polymer chain the regularity and size of the pores decrease. From this we suppose that the strong deformation of structures in the sample DB3 (Fig. 6c) is probably caused by a decrease of the average wall thickness between hole structures. This can bring instability into the final spatial structure, which collapses during preparation of the thin layer because of the softness of the swollen polymer material.

In the case of samples spun from 1,4-dioxane we did not find an indication of structures, except for the sample DB3 (image 6d) exhibiting dense, worm-like formations with a characteristic lateral dimension of ca. 75 nm. This is explained by increased content of acrylonitrile units in DB3 compared to DB1 and DB2 which necessarily leads to increased unfavorable segmental interactions between PS and P(S-*co*-AN) blocks and enhanced interaction of acrylonitrile with dioxane.

After the tetrazolation process we performed the same AFM experiments with the modified polymers. In Fig. 7 are shown results obtained from samples spun from THF solutions. Organized structures appear for polymers DB1T (Fig. 7a) and DB2T3 (Fig. 7b and c). That sample with lower molecular weight (DB1T) presents an unclear structure similar to the non-tetrazolated system DB3 (Fig. 6c). In contrast to the non-tetrazolated polymer the regular structure of gaps is lost and the rims

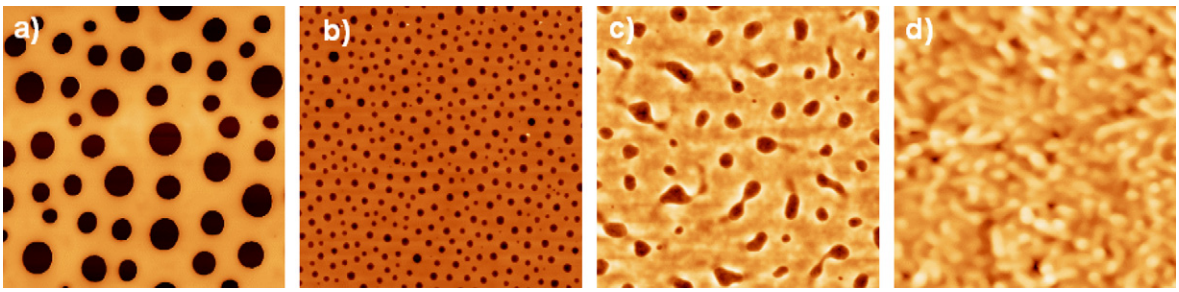

Fig. 6. Atomic force microscopy results for polymer: (a) DB1 cast from THF, 10 μm scan, topography, $Z = 225$ nm; (b) DB2 cast from THF, 10 μm scan, topography, $Z = 224$ nm; (c) DB3 cast from THF, 10 μm scan, topography, $Z = 95$ nm; (d) DB3 cast from dioxane, 1 μm scan, topography, $Z = 57$ nm.

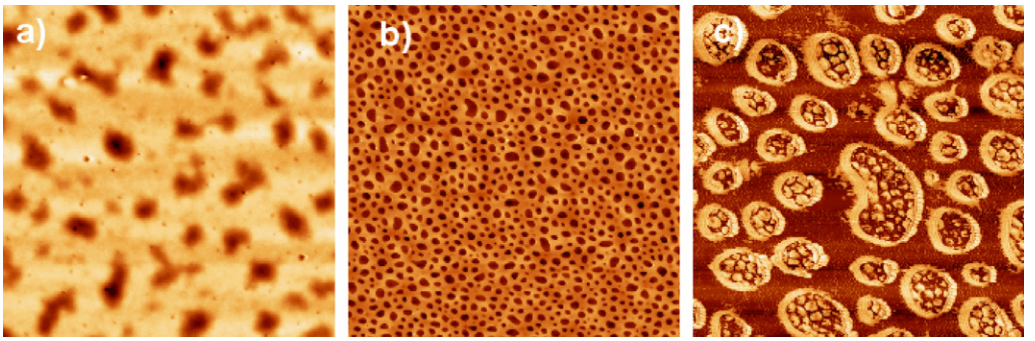

Fig. 7. Atomic force microscopy results for tetrazoled polymer: (a) DB1T, cast from THF, 5 μm scan, topography, $Z = 31$ nm; (b) DB2T3 cast from THF, 10 μm scan, topography, $Z = 264$ nm; (c) DB2T3 cast from THF, 2 μm scan, phase, $Z = 133°$.

are strongly deformed into shapes of average size ca. 500 nm. The system DB2T on the other hand shows well organized hole-like structures that are however different from those obtained from the unmodified polymer. The tetrazolated sample shows a strong hole formation with a much higher density of holes, the matrix between holes is much thinner, and the shape of the holes is deformed. This structure differs from the previous one not only by the topographical configuration but also by the fact that at the bottom side of the observed holes appears an indication of a fine terrace substructure. This substructure with diameter of 50–70 nm is clearly visible also in the phase scan in Fig. 7c.

AFM scans for tetrazolated polymers DB2T3 (image a and b) and DB3T (image c and d) spun from dioxane are shown in Fig. 8. The samples of tetrazolated DB2T3 demonstrate an indication of lamellar formations with a good contrast both in topography and phase scans. The characteristic dimension of the lamellar structures is approximately 70 nm being in good agreement with domain spacing obtained by SAXS and TEM experiments. The samples of DB3T again – as in the case of unmodified polymer – demonstrate worm-like formations with unclear boundaries. This can be a projection of deformed cylindrical or cubic formations with average diameter of ca. 50 nm, as is visible in the phase scan in Fig. 8d.

The obtained results show that the tetrazolation process brings into the polymer chains new incompatible sections with the ability to self-organize at the boundary of microphase separated domains. Experimentally, we also confirmed the generally accepted fact that the structure of thin layers of block copolymers is strongly influenced by the interaction with solvents [62–64]. This was demonstrated by using two ethers – THF and 1,4-dioxane – to prepare solutions of non-modified and tetrazolated copolymers. The influence of composition of the blocks (the ratio of styrene/acrylonitrile/nitrogen content) on the self-assembly of examined samples is also very important. From the results we can conclude that for the non-tetrazolated polymer samples prepared from THF the ability to form holes and the dimension and regularity of these holes decrease with decreasing length of the styrene block and also with increasing content of acrylonitrile (AN) in the

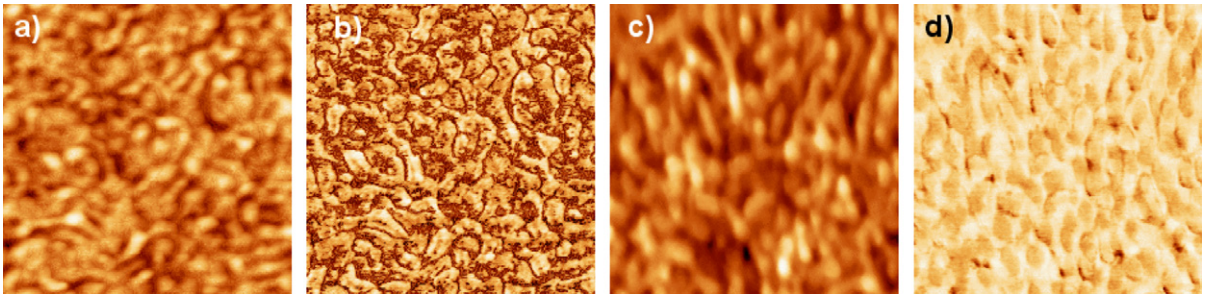

Fig. 8. Atomic force microscopy results for tetrazoled polymer: (a) DB2T3 cast from dioxane, 1 μm scan, topography, $Z = 9$ nm; (b) phase image of the (a), $Z = 98°$; (c) DB3T cast from dioxane, 1 μm scan, topography, $Z = 22$ nm (d) phase image of the (c), $Z = 51°$.

second block. Comparing the polymers DB2 and DB3 that have similar M_w and differ mainly in AN content we see that the fraction of the AN in the molecule has a stronger effect than the other parameters. When using dioxane to prepare thin layers of the non-tetrazolated polymers we did not obtain noticeable surface formations and the surface remained smooth. Only for the sample with higher molecular weight (DB3) we observed a kind of phase separation into the disordered lamellae or cylinders. After tetrazolation we obtained a series of very individual results because of variable degree of tetrazolation of the AN-containing block. For films cast from THF solutions, the increasing of level of tetrazolation increases the ability to form structures since it increases the incompatibility between the two blocks. The same situation exists also for dioxane solutions, where the more modified samples demonstrate highly organized hole formations. The other, less tetrazolated samples, does not show a structure formation or have just a weak ability to form self-assembled domains.

4. Conclusion

In this contribution we have described the synthesis of PS-*b*-PSAN block copolymers with different composition and content of acrylonitrile. The fraction of the neat polystyrene block was in the range 35–65%. We have shown that the morphology of the original polymer is lamellar. This demonstrates that this polymer which has one block of type A and the other block is a random mixture of A and B, behaves from a thermodynamic point of view as a classical diblock copolymer A-*b*-B. We have also successfully modified the polymer by tetrazolation of the acrylonitrile units to various degrees. After tetrazolation, the morphology of the polymer remained lamellar, but the lamellar period increases with increasing degree of tetrazolation.

Light scattering from THF solutions of these polymers shows that the original polymers are fully dissolved, while for the tetrazolated versions there is always a certain fraction of clusters present in the solutions. This demonstrates that the tetrazolation is a random process yielding certain chains with a larger degree of modification. These then aggregate in clusters while chains with a lower degree of tetrazolation remain fully dissolved. This behavior in solution is important in applications where thin films are produced. We have shown by the AFM technique that more pronounced surface organization into hole-like structures was obtained in the case of tetrazolated polymers.

Acknowledgements

The authors gratefully acknowledge support by the Grant Agency of the Czech Republic (SON/06/E005) within the EUROCORES Programme SONS of the European Science Foundation, which is also supported by the European Commission, Sixth Framework Programme. D.G. acknowledges the Marie Curie Fellowship at the Institute of Macromolecular Chemistry in Prague, under contract No. HPMT-CT-2001-00396. The authors thank Dr. M. Slouf of IMC for providing the TEM images.

References

[1] Hawker CJ, Bosman AW, Harth E. Chem Rev 2001;101:3661.
[2] Matyjaszewski K, Xia J. Chem Rev 2001;101:2921.
[3] Moad G, Rizzardo E, Thang SH. Aust J Chem 2005;58:379.
[4] Fukuda T, Terauchi T, Goto A, Tsujii Y, Miyamoto T, Shimizu Y. Macromolecules 1996;29:3050.
[5] Benoit D, Chaplinski V, Braslau R, Hawker CJ. J Am Chem Soc 1999;121:3904.
[6] Detrembleur C, Sciannamea V, Koulic C, Claes M, Hoebecke M, Jerome R. Macromolecules 2002;35:7214.
[7] Tsarevsky NV, Sarbu T, Göbelt B, Matyjaszewski K. Macromolecules 2002;35:6142.
[8] Lazzari M, Chiantore O, Mendichi R, Lopez-Quintela MA. Macromol Chem Phys 2005;206:1382.
[9] Pietrasik J, Dong H, Matyjaszewski K. Macromolecules 2006;39:6384.
[10] Chiefari J, Chong YK, Ercole F, Krstina J, Jeffery J, Le TPT, et al. Macromolecules 1998;31:5559.
[11] Fan D, He J, Xu J, Tang W, Liu Y, Yang Y. J Polym Sci Part A: Polym Chem 2006;44:2260.
[12] Baumert M, Mülhaupt R. Macromol Rapid Commun 1997;18:787.
[13] Baumann M, Roland AI, Schmidt-Naake G, Fischer H. Macromol Mater Eng 2000;280:1.
[14] Lokaj J, Brozova L, Holler P, Pientka Z. Collect Czech Chem Commun 2002;67:267.
[15] Leiston-Belanger JM, Penelle J, Russel TP. Macromolecules 2006;39:1766.
[16] Ermakov V, Rebrov AI, Litmanovich AD, Plate NA. Macromol Chem Phys 2000;201:1415.
[17] Litmanovich A, Plate NA. Macromol Chem Phys 2000;201:2176.
[18] Gupta ML, Gupta B, Oppermann W, Hardtmann GJ. Appl Polym Sci 2004;91:3127.
[19] Kopic M, Flajsman F, Janovic Z. J Macromol Sci Chem 1978;1:17.
[20] Hseish DT, Schulz DN, Peiffer DG. J Appl Pol Sci 1995;56:1673.
[21] Hseish DT, Peiffer DG. J Appl Pol Sci 1995;56:1667.

[22] Schmidt-Naake G, Becker H, Becker W. Angew Makromol Chem 1999;267:63.
[23] Schmidt-Naake G, Carbera A. Macromol Chem Phys 2004;205:95.
[24] Todorov NG, Valkov EN, Stoyanova MG. J Pol Sci Part A: Polym Chem 1996;34:863.
[25] Ko YG, Choi US, Park YS, Woo JW. J Pol Sci Part A: Pol Chem 2004;42:2010.
[26] Carneiro Riqueza E, Palermo de Aguiar A, Claudio de Santa Maria L, Palermo de Aguiar MRM. Polym Bull 2002;48:407.
[27] Gaponik PN, Ivashkevich OA, Karavai VP, Lesnikovich AI, Chernavina NI, Sukhanov GT, et al. Ang Makromol Chem 1994;219:77.
[28] Gaponik PN, Ivashkevich OA, Chernavina NI, Lesnikovich AI, Sukhanov GT, Gareev GA. Ang Makromol Chem 1994;219:89.
[29] Huang ME, Li XG, Li SX, Zhang W. React Funct Polym 2004;59:53.
[30] Ulbricht M, Hicke HG. Ang Makromol Chem 1993;210:69.
[31] Paton RM, Stobie I, Mortier RM. J Pol Sci Lett Ed 1982;20:573.
[32] Huisgen R. In: Padwa A, editor. 1,3-Dipolar cycloaddition chemistry. New York: Wiley; 1984. p. 1.
[33] Kolb HC, Finn MG, Sharpless KB. Angew Chem Int Ed 2001;40:2004.
[34] Bock VD, Hiemstra H, van Maarseveen JH. Eur J Org Chem 2006:51.
[35] Rostovtsev VV, Green LG, Fokin VV, Sharpless KB. Angew Chem Int Ed 2002;14:41.
[36] Díaz DD, Punna S, Holzer P, McPherson AK, Sharpless KB, Fokin VV, et al. J Polym Sci Part A: Polym Chem 2004;42:4392.
[37] Link AJ, Tirrell DA. J Am Chem Soc 2003;125:11164.
[38] Link AJ, Vink MKS, Tirrell DA. J Am Chem Soc 2004;126:10598.
[39] Wu P, Feldman AK, Nugent AK, Hawker CJ, Scheel A, Voit B, et al. Angew Chem Int Ed 2004;43:3928.
[40] Helms B, Mynar JL, Hawker CJ, Fréchet JMJ. J Am Chem Soc 2004;126:15020.
[41] Opsten JA, van Hest JCM. Chem Commun 2005:57.
[42] Joralemon MJ, O'Reilly RK, Matson JB, Nugent AK, Hawker CJ, Wooley KL. Macromolecules 2005;38:5436.
[43] Englert BC, Bakbak S, Bunz UHF. Macromolecules 2005;38:5868.
[44] Tsarevsky NV, Sumerlin BS, Matyjaszewski K. Macromolecules 2005;38:3558.
[45] Gao H, Matyjaszewski K. Macromolecules 2006;39:4960.
[46] Altintas O, Yankul B, Hizal G, Tunca U. J Pol Sci Part A: Pol Chem 2006;44:6458.
[47] Altintas O, Hizal G, Tunca U. J Pol Sci Part A: Pol Chem 2006;44:5699.
[48] Tsarevsky NV, Bernaerts KV, Dufour B, Du Prez FE, Matyjaszewski K. Macromolecules 2004;37:9308.
[49] Sumerlin BS, Tsarevsky NV, Louche G, Lee RY, Matyjaszewski K. Macromolecules 2005;38:7540.
[50] Malkoch M, Schleicher K, Drockenmuller E, Hawker CJ, Russel TP, Wu P, et al. Macromolecules 2005;38:3663.
[51] Parrish B, Breitenkamp RB, Emrick T. J Am Chem Soc 2005;127:7404.
[52] Lecomte P, Riva R, Schmeits S, Rieger J, van Butsele K, Jérôme K, et al. Macromol Symp 2006;240:157.
[53] Coady DJ, Bielawski ChW. Macromolecules 2006;39:8895.
[54] Lutz JF, Börner HG, Weichenhan K. Macromol Rapid Commun 2005;26:514.
[55] Lutz JF, Börner HG, Weichenhan K. Macromolecules 2006;39:6376.
[56] Pu HT, Ye S. React Funct Polym 2006;66:856.
[57] Kizhnyaev VN, Vereshchagin LI. Russ Chem Rev 2003;72:143.
[58] Kizhnyaev VN, Pokatilov FA, Vereshchagin LI, Smirnov AI. Proceedings of the 23rd discussion conference – Current and future trends in polymeric materials, 26–30 June, Prague; 2005.
[59] Jakeš J. Collect Czech Chem Commun 1995;60:1781.
[60] Benoit H, Higgins J. Polymers and neutron scattering. Oxford: Oxford University Press; 1997.
[61] Stepanek P. In: Brown W, editor. Dynamic light scattering: the method and some applications. Oxford: Oxford University Press; 1993.
[62] Kim G, Libera M. Macromolecules 1998;31:2569.
[63] Kim G, Libera M. Macromolecules 1998;31:2670.
[64] Černoch P, Štěpánek P, Pleštil J, Šlouf M, Sidorenko A, Stamm M. Eur Polym J 2007;43:1144.